



HAL
open science

Modeling of a new SMA micro-actuator for active endoscopy applications.

Joël Abadie, Nicolas Chaillet, C. LExcellent

► **To cite this version:**

Joël Abadie, Nicolas Chaillet, C. LExcellent. Modeling of a new SMA micro-actuator for active endoscopy applications.. *Mechatronics*, 2009, 19 (4), pp.437-442. 10.1016/j.mechatronics.2008.11.010 . hal-00380883

HAL Id: hal-00380883

<https://hal.science/hal-00380883>

Submitted on 4 May 2009

HAL is a multi-disciplinary open access archive for the deposit and dissemination of scientific research documents, whether they are published or not. The documents may come from teaching and research institutions in France or abroad, or from public or private research centers.

L'archive ouverte pluridisciplinaire **HAL**, est destinée au dépôt et à la diffusion de documents scientifiques de niveau recherche, publiés ou non, émanant des établissements d'enseignement et de recherche français ou étrangers, des laboratoires publics ou privés.

MODELING OF A NEW SMA MICRO-ACTUATOR FOR ACTIVE ENDOSCOPY APPLICATIONS

J. Abadie * N. Chaillet * C. LExcellent **

* *Automatique et Systèmes Micro-Mécatroniques*

** *Département Mécanique appliquée*

Institut FEMTO-ST UMR CNRS 6174

UFC / ENSMM / UTBM

24, rue Alain Savary, 25000 Besançon (FRANCE)

Abstract: Shape Memory Alloys (SMA) are good candidates to actuate endoscope heads but the cooling problem must be solved particularly in confined situations. For these reasons, a new SMA micro-actuator specially designed for active endoscopy applications has been developed in our laboratory. This work is a new step in the approach of using integrated thermoelectric cooling with SMA actuators. In fact, the Peltier effect is very attractive in such a case because this reversible phenomenon reduces the overheating of the external environment and provides forced cooling that decreases the response time. In this paper the actuator design and its working principle are presented. A fine modeling of the coupled mechanical and thermal behaviors gives a better understanding of the physical phenomenon involved in the actuator. Finally an experimental prototype has been developed and tested in order to verify the model predictions.

Keywords: Shape memory alloys, active endoscopy, thermo-electricity, modeling.

1. INTRODUCTION

Microtechnology and microsystems engineering require new active materials. These materials are often used to develop micro-actuators and micro-sensors. In this category of materials, Shape Memory Alloys (SMAs) are good candidates for micro-actuation. SMA wires, or thin plates, can actuate microrobots and are able to provide very significant forces, but have low dynamic response. These materials are often used to actuate hydro-foils or for underwater propulsion applications, where cooling environment is relevant (Yonghua *et al.*, 2005; Shinjo and Swain, 2004; Rediniotis *et al.*, 2002; Ono *et al.*, 2004). These structures are based on adjacent vertebrae segments actuated by SMAs. Other similar structures have been designed to reproduce artificial fingers or

bio-inspired caterpillar locomotion (Kyu-Jin and Asada, 2005; Trimmer *et al.*, 2006). The actuation is there performed in a low capabilities cooling environment compared to the water environment. It produces unexpected behaviour and low dynamic response. A technic consist in using thermoelectric coolers (Kyu-Jin and Asada, 2005).

The control of the SMA phases transformations, and then the mechanical power generation, is driven by the temperature of the material. Classically Joule effect is an easy way to heat the SMA actuators, but cooling is made by an other way (typically by natural convection or conduction). Unfortunately, endoscopic applications involve confined environments with a low convection capabilities and a variable external temperature.

Moreover, the dynamic response of the actuator depends on cooling capabilities. The work of J. Szweczyk *et al.* shows the difficulties to cool the SMA when it is integrated in a flexible head (Szweczyk *et al.*, 2001). For these reasons, we have examined a reversible way of heating and cooling SMA micro-actuators, based on the thermoelectric effect, e.g. the Peltier effect.

Even if it is often bad known and rarely used, the implementation of thermoelectric elements has already been performed for the temperature control of shape memory alloys. Several investigations and developments that use thermoelectric coolers in this field have shown that it can work efficiently (Thrasher *et al.*, 1992; Semenyuk *et al.*, 1998; Khan *et al.*, 2003). In these particular cases, the SMA actuator and the thermoelectric cooler are separated and calorific energy exchanges, between them, are done by thermal conduction. However, it seems that the best results are obtained, when choosing the maximal integration of the thermoelectric phenomenon (Bhattacharyya *et al.*, 1995; Lagoudas and Ding, 1995). In this case, the thermoelectric connections are directly made on the SMA element. A thermal model has already been validated by an experimental thermoelectric system which is described in a previous paper (Abadie *et al.*, 1999). The development of a basic thermoelectric actuator in our laboratory has demonstrate the interest of the Peltier effect in temperature control of NiTi (Abadie *et al.*, 2002). The goal of the present paper is to describe and model a new thermoelectric SMA micro-actuator specially designed for endoscopic applications.

2. ACTUATOR DESCRIPTION

2.1 General description

The developed actuator is composed of two elementary stages symmetrically assembled (see figure 1). Each stage is sequentially composed of a copper semi-ring, a Bi_2Te_3 N doped ingot, a NiTi blade, a Bi_2Te_3 P doped ingot and a second copper semi-ring. Finally, the actuator dimensions are: 4 mm in diameter, 9 mm in length and the NiTi blade itself has 200 μm in thickness.

When the actuator is supplied with a 0.6 A current, the blades are bending. They produce a measured angle θ of about 25° . When the current is inverted, a symmetric deflection is obtained. The reached deflection after the current application is maintained even when the current is removed. To obtain this kind of behavior, we had to design the actuator with a special blade configuration with a thermal control performed by an integrated

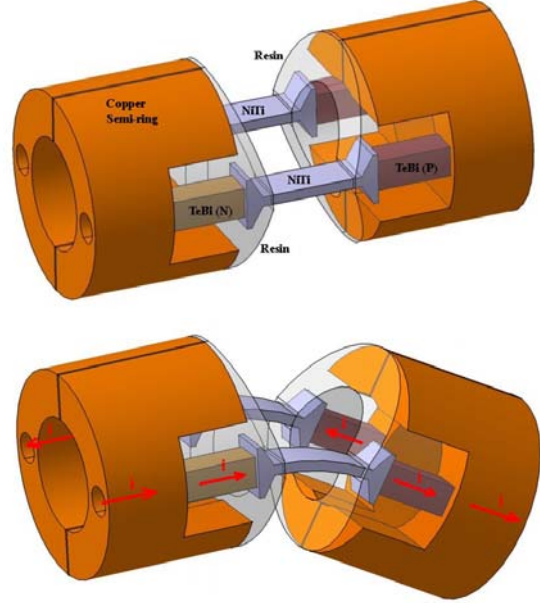


Fig. 1. Actuator constitution (up), electrically supplied actuator (down).

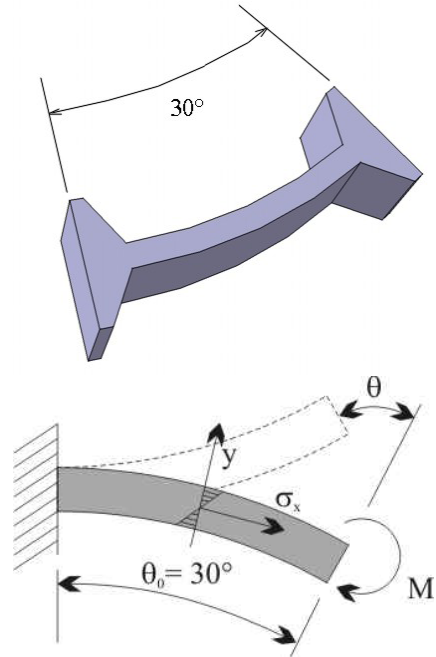


Fig. 2. Niti blade in austenite phase (up), blade model parameters (down).

Peltier system. So, the phase transformation of the SMA blades is driven by the heat transfers produced by the thermoelectric system.

2.2 Mechanical principle

In the actuator, the two blades have an antagonist behaviour. First, the blades are machined with an initial curvature of 30° (corresponding to the shape in the austenitic phase), in a SMA material for which the temperature transforma-

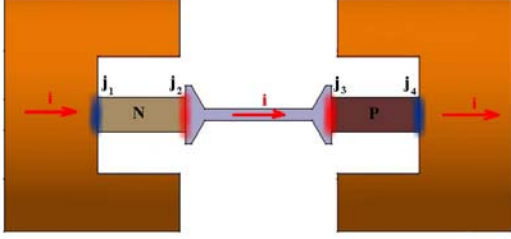


Fig. 3. Thermoelectric principle in an elementary stage.

tion is above the room temperature (see figure 2). Then they are anti-symmetrically positioned in the actuator such as when a blade is heated to austenite, its shape memory effect occurs and produces a martensite reorientation in the cold antagonist blade (push-pull working). Only one blade can be heated at the same time. One way displacement is obtained by heating the first blade and the reverse displacement by the second one. In this configuration the actuated blade is not able to completely reorient the other blade (not actuated). For this reason, the displacement range is lower than 60° . Practically a range of 40° is possible when the austenite phase transformation is completed in a blade.

2.3 Thermoelectric system

The maximum integration of the thermoelectric system consists in placing thermoelectric junctions directly between the copper semi-rings, the TeBi ingots and the NiTi blade in each elementary stage. By this way, four junctions j_1, \dots, j_4 are activated by the going through current (see figure 3). For a positive current i , the junctions j_1 and j_4 produce heat while j_2 and j_3 absorb heat. If i is negative, heat production/absorption is inverted due to the fact that the Peltier effect is a reversible phenomenon.

3. ACTUATOR MODELING

With this SMA actuator, complex thermo-mechanical coupling effects must be taken into account. To simplify, we have split the study in two parts. First, the mechanical behavior of one NiTi blade is investigated in order to determine the stress, the strain and the mechanism of the phase transformation for bending. Then, thermal modeling for temperature prediction is performed considering the blade as a passive material and the thermoelectric system in a global point of view.

3.1 SMA bending model

A phenomenological approach is used to model the SMA blade in order to predict its behavior by using the actual physical knowledge and the associated equations that provide the material physicists (Leclercq and LExcellent, 1996). The chosen approach is based on the Helmholtz free energy expression of the different phases mixture: austenite, self accommodating martensite and stress induced martensite (Benzaoui *et al.*, 1997). This approach gives an one-dimension prediction of the SMA behavior, e.g. when and how phase transformation occurs under thermal and strain solicitations. Bending is solved by using a spatial discretization of the blade. The present paper does not give the details of this modelling. For more details please refer to (Abadie *et al.*, 2004). To summarize, the blade is considered as a stack of thin Niti layers. The one-dimension model is applied at each layer assuming that the layer strain $\varepsilon_x(y)$ situated at the distance y of the neutral axis is:

$$\varepsilon_x(y) = \frac{y\theta}{l} = yk \quad (1)$$

where l is the blade length, θ is its extremity rotation angle and k its curvature assuming a circular bending (see figure 2). The stress in the layer is calculated using:

$$\sigma_x(y) = E(\varepsilon_x(y) - \gamma z_\sigma(y)) \quad (2)$$

where γ and z_σ are respectively the SMA maximum pseudo-plastic deformation and the volume fraction of stress induced martensite. The term including these two parameters corresponds to the pseudo-plastic strain induced by the presence of the stress induced martensite. E is the average Young modulus of the material. The heat equation used to determine the temperature T of the blade is:

$$\rho(c_v \dot{T} - \Delta u \dot{z}) = q + \lambda \Delta T \quad (3)$$

where Δu , q , λ , z and ΔT are respectively the phase transformation latent heat, the thermal power applied, the thermal conductivity, the total volume fraction of martensite (e.g. volume fraction of self accommodating martensite z_t + stress induced martensite z_σ), and the temperature laplacian. We use a classic heat equation where is added the term $\Delta u \dot{z}$ corresponding to the heat produced or absorbed by the phase transformation. This heat is correlated to the variation of the volume fraction of martensite.

We have used Matlab/Simulink to calculate the model response in the case of a blade of 2 mm in

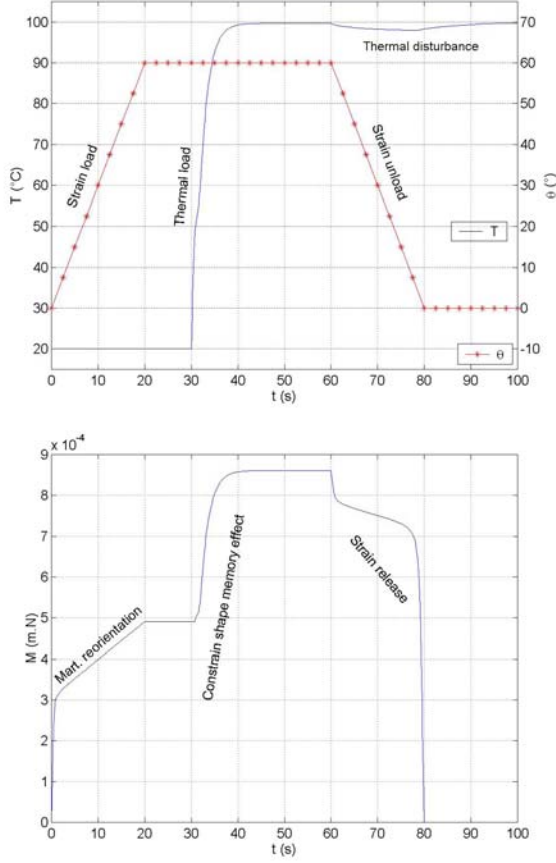


Fig. 4. Model input signals (up), calculated bending momentum (down).

length, 0.8 mm in wideness, 0.2 mm in thickness and with an initial angle $\theta_0 = 30^\circ$. The stress free state austenite and martensite start temperatures are respectively $A_s = 52^\circ\text{C}$ and $M_s = 38^\circ\text{C}$, the maximum pseudoplastic deformation is $\gamma = 0.05$, the latent heat is $\Delta u = 20652 \text{ J.kg}^{-1}$. In this model, the input are the thermal power q and the rotation angle θ . The natural convection and Joule effect are the two physical phenomenon introduced in q . The room temperature and self accommodating martensite fraction z_t are taken as the initial conditions of the blade. The simulation consists in applying an imposed strain, a thermal load and a strain unload (see figure 4 (up)). The strain is imposed through θ .

The imposed strain load occurs at the beginning of the simulation and has 20 s of duration. It corresponds to the martensite reorientation process. The bending momentum M increases and reaches $M_r = 4.9 \cdot 10^{-4} \text{ N.m}$. At $t = 20 \text{ s}$, the stress distribution is shown on figure 5 (up). During the load, the martensite volume fractions remains equal to 1. At $t = 30 \text{ s}$, the thermal load occurs and generates the phase transformation. It begins from the blade skin and spreads to the neutral fiber (see figure 5 (down) and 6 (up)). At $t = 60 \text{ s}$, the

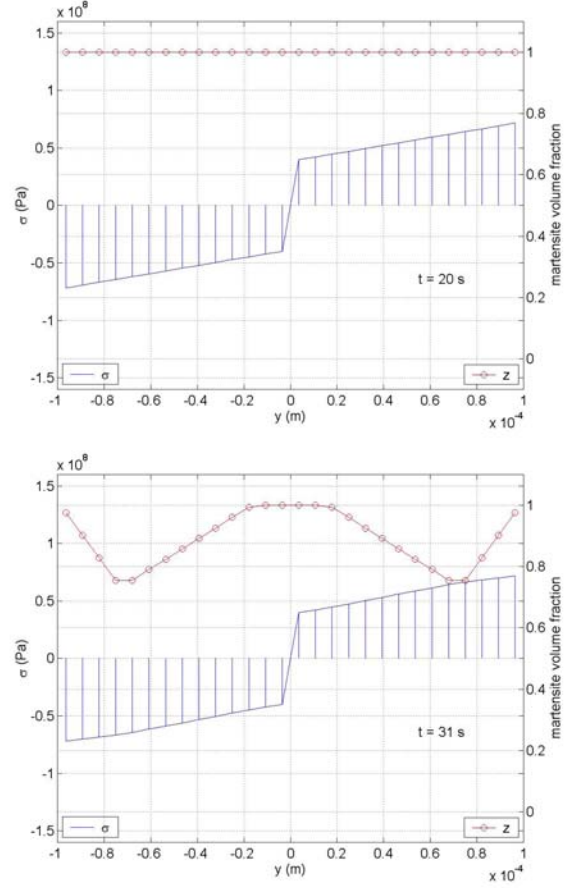


Fig. 5. Martensite and stress evolution during thermal load.

constrained memory effect bending momentum M reaches $M_c = 8.6 \cdot 10^{-4} \text{ N.m}$. Consequently the useful momentum for the actuator is the difference between M_c and M_r . At $t = 60 \text{ s}$, the strain unload occurs which induces the martensite transformation and produces a thermal disturbance (see figure 4 (up)). The calculated rotation angle is then $\theta_u = 3^\circ$ when the bending momentum is equal to M_r . In fact, the actuator useful range is $\theta_{max} = 54^\circ$.

3.2 Modeling of the complete thermoelectric system

To determine the thermal behavior of the actuator, one has to consider the copper rings, the TeBi ingots and the SMA blades (let us note that the SMA latent heat is not involved in the reorientation process):

$$\rho c_v \dot{T} = q + \lambda \Delta T \quad (4)$$

The internal heat source q is zero for the rings and $q = \rho_e j^2$ for the ingots and the blades. The thermal conductivity λ , the electric resistance ρ_e and the material density ρ are given in the table 1.

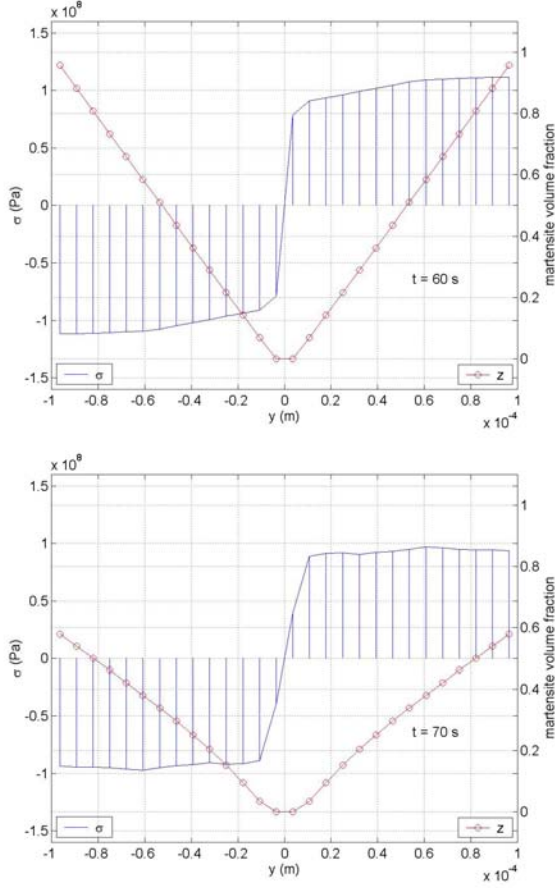


Fig. 6. Martensite and stress evolution during mechanical unload.

Table 1. Thermal parameters.

	ρ_e ($\Omega.m$)	ρ ($kg.m^{-3}$)	λ ($W.m^{-1}.K^{-1}$)
Copper	0	8700	400
NiTi	$6.3 \cdot 10^{-7}$	6500	22
TeBi	8.10^{-6}	7530	1,61

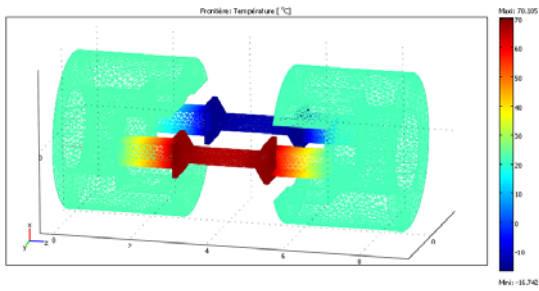


Fig. 7. Stationary state solution.

The Peltier effect is taken into account as a heat flux discontinuity ϕ in the junctions between copper, TeBi and NiTi. This heat flux is:

$$\phi_{j_1,j_4} = \pi j \quad \text{and} \quad \phi_{j_2,j_3} = -\pi j \quad (5)$$

where π is the Peltier coefficient of the ingots ($\pi = 5.3 \cdot 10^{-2}$ Volt).

The equations are solved using the 3D heat transfer by conduction module from Comsol Multi-

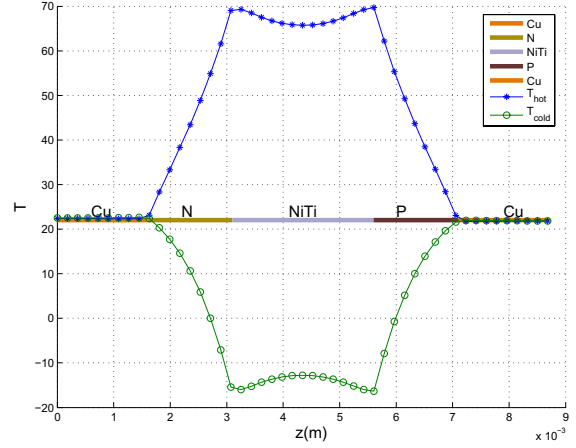


Fig. 8. temperature distribution along the two thermo-electric ways.



Fig. 9. Developed actuator.

physics. The boundaries conditions are set as a natural convection with a heat transfer coefficient $h = 280 W.m^{-2}$ and a room temperature of $22^\circ C$. The current applied to the actuator is $i = 0.6 A$. The steady state solution shows an homogeneous temperature in the blades and in the copper rings (see figure 7). A closer look at the temperature curve, taken along an axis going through the NiTi blade from the left copper ring to the right one (the thermo-electric way), show a temperature gradient of about $4^\circ C$ in the hot and the cold blades. Due to the heat dissipated by Joule effect in the thermo-electric ingots, the T_{hot} and T_{cold} curves are not symmetric around the room temperature. Moreover the rings temperature remains at the room temperature and only the blades are heated and cooled. The reached temperature is $68^\circ C$ for the hot blade and $-15^\circ C$ for the cold one (see figure 8).

4. EXPERIMENTAL RESULTS

An experimental actuator has been made and tested in order to validate the simulation results (see figure 9). The temperature measurements have been made using Chromel/Alumel microthermocouples with $25 \mu m$ in diameter wires. A first thermocouple was glued on the left copper ring to measure T_{Cu} . Two other thermocouples

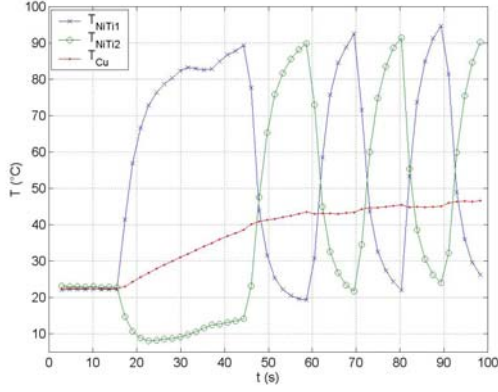


Fig. 10. Temperature measurement under current steps.

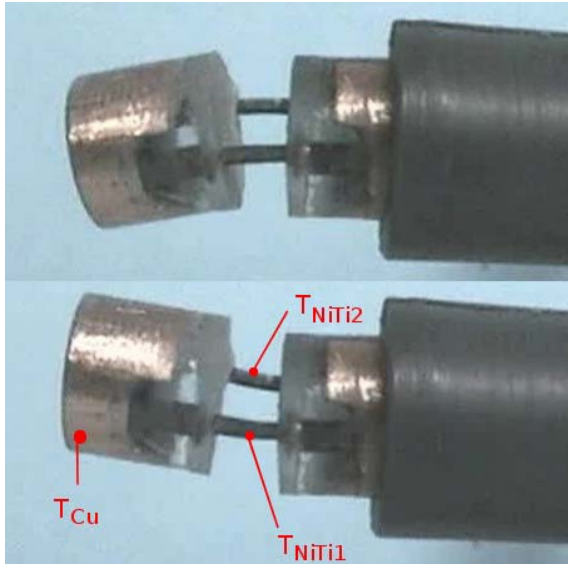


Fig. 11. Position for $i = 0,6$ A (up) and $-0,6$ A (down)

were glued in the middle of each NiTi blade to measure T_{NiTi1} and T_{NiTi2} (see figure 11). Figure 10 shows the temperature evolution under current steps. At the beginning of the measurement, when no current is applied the three thermocouples indicates the room temperature (22°C). At $t = 16$ s, a current step of $0,6$ A produces respectively in the blade 1 and 2 a temperature increase and decrease as predicted by the simulation. At $t = 45$ s, the current is set to $-0,6$ A and so on. In the same time, the copper temperature slowly increases and finally reaches 46°C . This unwanted phenomenon is probably due to a lower convection than the model estimation but mainly to a high contact resistance (which increases the Joule effect) in the thermoelectric junctions of the tested prototype.

The simulation has been modified in order to take into account this resistance. At the Peltier heat flux, a contact resistance heat flux has been added to the eight thermo-electric junctions as follow :

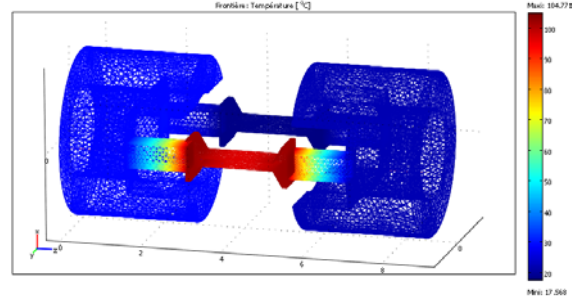


Fig. 12. stationary state solution with a contact resistance.

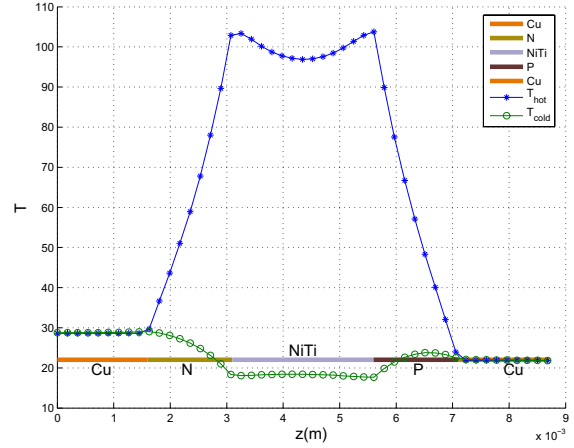


Fig. 13. temperature distribution along the thermo-electric branch with contact resistance.

$$\phi_{j_1,j_4} = \pi j + r_c j^2 \quad \text{and} \quad \phi_{j_2,j_3} = -\pi j + r_c j^2 \quad (6)$$

where r_c is the contact resistance. According to the experiments, the value of r_c has been set to $1,1 \cdot 10^{-8} \Omega \cdot \text{m}^2$. In this case, the steady state response of the model show a better accuracy with the experiments (see figure 12 and 13). The temperature of the cold blade reach a minimum value of 18°C . The simulation show a temperature T_{Cu} of the left ring equal to 29°C while the experimental value is around 45°C at steady state. This phenomenon is probably due to the limit conditions taken for the connection of the actuator to the fixed support. In the model, the temperature of the ring face in contact with the support is fixed to the room temperature. In fact, this support is made of plastic which has low thermal conductivity. As a result, the temperature of this face won't remain to 22°C but will increase. No further investigations have been made on this particular point.

The important result is that a particular attention is required to make the solders between the TeBi ingots and the others elements to avoid that the Joule effect became preponderant in front of the Peltier effect in the thermo-electric junctions.

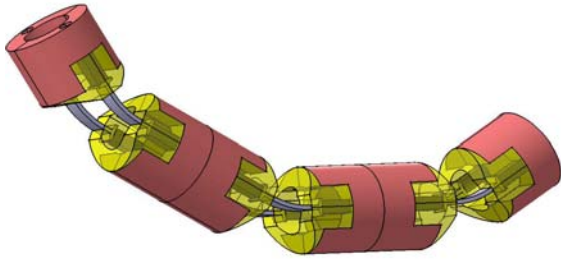


Fig. 14. Multi stage endoscope head.

At the moment, our soldering method should be reviewed.

The experimental rotation range was measured from video acquisition (see figure 11). The above picture is taken when the current is 0,6 A, after transient movement, the below one when the current is inverted. This actuator has a multi-stable property. This means that when the current is canceled, the actuator rotation angle remains constant. It is necessary to apply the current only during the moving phases in the reachable range.

The reachable range is 25° , a low value according to the $\theta_{max} = 54^\circ$ of the model prediction. This may be due to a bad choice in the active material: temperature transformation are in accordance with the model but the heat treatments performed on the blade have certainly provide lower plastic deformation than the 5% expected on classical NiTi material. The mechanical dynamic response is correlated to the temperature response of the blades. The test presented on figure 10 shows that cycling is possible at 0,05 Hz. If the frequency is increased it will decrease the maximum rotation range. One can note the it is also possible to supply only one elementary stage (or side) at a time. In this case the response time of the actuator is increased due to a slower martensite phase transformation (convection cooling only). For this actuator, there is no interest to supply one side at a time. The characteristics are better when the two sides are supplied simultaneously.

5. CONCLUSION AND PERSPECTIVES

This study shows that the use of SMA antagonist blades associated with an integrated thermoelectric system is efficient for active endoscopy applications. Because of a low heat dissipation provided by the air environment, the use of a thermo-electric system is very important to keep an efficient actuation with a low electric consumption. The dynamic response is reasonable even if faster responses can be obtained in water environment where convection is higher. The considered applications are mainly for air environments were

heat dissipation is a real problem.

The developed actuator can be improved by the use of a better NiTi alloy to obtain higher rotation angle. Our future work will consist in using several elementary stages electrically and mechanically interconnected to build a complete endoscope head with free space in its center for optical fibers and tools (see figure 14). Industrial or medical application are conceivable based on this work and could succeed in high technology systems.

REFERENCES

- Abadie, J., N. Chaillet and C. LExcellent (2002). An integrated shape memory alloy micro-actuator controlled by thermoelectric effect. *Sensors and Actuators A: Physical* **A99**(3), 297–303.
- Abadie, J., N. Chaillet and C. LExcellent (2004). Bending model of an integrated SMA micro-actuator. *Journal of Intelligent Material Systems and Structures* **15**(8), 601–609.
- Abadie, J., N. Chaillet, C. LExcellent and A. Bourjault (1999). Thermoelectric control of shape memory alloy microactuator : a thermal model. In: *Proc. of SPIE Smart Structures and Materials*. Vol. 3667. Newport Beach CA USA. pp. 326–336.
- Benzaoui, H., C. LExcellent, N. Chaillet, B. Lang and A. Bourjault (1997). Experimental study and modeling of a TiNi shape memory alloy wire actuator. *Journal of Intelligent Material Systems and Structures* **8**(7), 619–629.
- Bhattacharyya, A., D. Lagoudas, Y. Wang and K. Kinra (1995). On the role of thermoelectric heat transfer in the design of SMA actuators: theoretical modeling and experiment. In: *Smart Mater. Struc..* Vol. 4. pp. 252–263.
- Khan, M., D. Lagoudas and O. Rediniotis (2003). Thermoelectric SMA actuator: preliminary prototype testing. In: *Proceedings of SPIE, Smart Structures and Materials*. Vol. 5054. pp. 147–155.
- Kyu-Jin, Cho and H. Asada (2005). Multi-axis sma actuator array for driving anthropomorphic robot hand. In: *Proceedings of International Conference on Robotics and Automation ICRA*. pp. 1356–1361.
- Lagoudas, D. and Z. Ding (1995). A modeling of thermoelectric heat transfert in shape memory alloy actuators : transient and multiple cycle solutions. In: *International Journal of Engineering Science*. Vol. 33(15). p. 2345.
- Leclercq, S. and C. LExcellent (1996). A general macroscopic description of the thermo-mechanical behavior of shape memory alloys. *J. Mech. Phys. Solids* **44**(6), 953–980.

- Ono, Nagato, Masahiro Kusaka, Minoru Taya and Chiyan Wang (2004). Design of fish fin actuators using shape memory alloy composites. In: *Proc. SPIE*. Vol. 5388. pp. 305–312.
- Rediniotis, O.K., L.N. Wilson, D.C. Lagoudas and M.M. Khan (2002). Development of a shape-memory-alloy actuated biomimetic hydrofoil. *Journal of Intelligent Material Systems and Structures* **13**(1), 35–49.
- Semenyuk, V., S. Seelecke, J. Stockholm and A. Musolff (1998). The use of thermoelectric cooling for shape memory wire temperature control. In: *Proc. of ECT' 98*.
- Shinjo, N. and G.W. Swain (2004). Use of a shape memory alloy for the design of an oscillatory propulsion system. *IEEE Journal of Oceanic Engineering* **29**(3), 750–755.
- Szewczyk, J., V. de Sars, P. Bidaud and G. Dumont (2001). An active tubular polyarticulated micro-system for flexible endoscope. *Lecture Notes in Control and Information Sciences* **271**, 179 – 188.
- Thrasher, M., A. Shahin, P. Meckl and D. Jones (1992). Thermal cycling of shape memory alloy wires using semiconductor heat pump modules. In: *Fisrt European Conf. On Smart Structures and materials*. Glasgow.
- Trimmer, B.A., A.E. Takesian, B.M. Sweet, C.B. Rogers, D.C. Hake and D.J. Rogers (2006). Caterpillar locomotion: A new model for soft-bodied climbing and burrowing robots. In: *7th International Symposium on Technology and the Mine Problem*.
- Yonghua, Z., L. Shangrong, M. Ji and Y. Jie (2005). Development of an underwater oscillatory propulsion system using shape memory alloy. In: *International Conference Mechatronics and Automation*. Vol. 4. pp. 1878–1883.